STRESSES AND DEFLECTIONS OF CANTILEVERED FIBERGLASS REINFORCED PLASTIC BEAMS

by

George Michael Meza

A Thesis Submitted to the Faculty of the

DEPARTMENT OF CIVIL ENGINEERING AND ENGINEERING MECHANICS

In Partial Fulfillment of the Requirements
For the Degree of

MASTER OF SCIENCE
WITH A MAJOR IN CIVIL ENGINEERING

In the Graduate College

THE UNIVERSITY OF ARIZONA

1 9 7 0

STATEMENT BY AUTHOR

This thesis has been submitted in partial fulfillment of requirements for an advanced degree at The University of Arizona and is deposited in the University Library to be made available to borrowers under rules of the Library.

Brief quotations from this thesis are allowable without special permission, provided that accurate acknowledgment of source is made. Request for permission for extended quotation from or reproduction of this manuscript in whole or in part may be granted by the head of the major department or the Dean of the Graduate College when in his judgement the proposed use of material is in the interest of scholarship. In all other instances, however, permission must be obtained from the author.

SIGNED: George M. Mays

APPROVAL BY THESIS DIRECTOR

This thesis has been approved on the date shown below:

Haaren A. Miklofsky
Professor of Civil Engineering

May 13 1970
Date

To my wife, Diane,

for her encouragement, patience

and help in writing this manuscript.

ACKNOWLEDGMENTS

The author wishes to express his deep gratitude to his thesis director, Professor Haaren A. Miklofsky, for his active interest, helpful guidance and suggestions.

Appreciation is also extended to Robert Musser of Dyna-Strux, Inc. for supplying materials and preparing test specimens.

TABLE OF CONTENTS

LIST OF ILLUSTRATIONS

LIST OF ILLUSTRATIONS--CONTINUED

LIST OF TABLES

ABSTRACT

This study concerns the development of a flexure and deflection equation for use in the design of fiberglass reinforced plastics. It also includes the tests that were run on beam specimens to compare the actual with the theoretical results.

The reinforcement used in the specimens was a woven fiber glass mat (a Pittsburg Plate Glass Company Product) while the matrix was made up of a polyester resin. A fiberglass reinforced plastic cantilevered beam was subjected to various concentrated loads, and the corresponding deflections and matrix strains were recorded. Three beam specimens having various thicknesses and orientations of reinforcing fibers were used in the testing. The results obtained by the experiments were compared to the corresponding answers derived by the new theory. It was found that the flexure formula gave answers whose average error was 6 percent, while the deflection results were within 4 percent.

CHAPTER I

INTRODUCTION

Reinforced plastics has been the subject of several books and numerous shorter treatments in its field; however, there is little information in these publications on design criteria for reinforced fiberglass plastics in a form in which a civil engineer may apply.[1*] In a review of the literature, it was noticed that although some design procedures are available for axial stress, there is no known publication that shows how to design a fiberglass reinforced plastic beam for flexure or deflection. Therefore, the author has chosen to concentrate on developing an analysis whereby the stresses and deflections of fiberglass reinforced plastic beams can be evaluated with reasonable accuracy.

Fundamental Concepts of Fiberglass Reinforced Plastics

"Fiberglass reinforced plastics," occasionally abbreviated as frp, implies that two materials, one consisting of a fiberglass reinforcement and the other a fiber impregnating matrix resin, are combined to obtain a composite material. This composite possesses many of the desirable characteristics of each constituent material.[2]

Fiberglass reinforcement encompasses a wide field of reinforcement. At one end of the spectrum are the short chopped fibers added to

---

* Superscript numbers are citation of references shown on page 56.

molding compounds to form such familiar shapes as boats, sports cars, and patio roofing to mention a few. At the opposite extreme are the high strength forms of woven cloth in which glass fibers provide reinforcement in two directions at right angles to each other. The latter type of reinforcing is the type of reinforcing that has been chosen as the subject of research for this thesis.

The bonding of these reinforcing fibers is accomplished by impregnation with any of several possible resins. The most common resins being used are the epoxies and the polyesters (thermosetting). The resin acts as a binding matrix to provide shape, stiffness, strength to hold the fibers together, and most of the volume. It also provides continuity between layers of fibers and protection for the fibers.[2] A thermosetting polyester resin was used throughout this study.

Using a woven cloth as the reinforcement and the polyester as the matrix, the resulting mechanical properties depend on the direction at which the load is applied. This composite, or laminate, is non-isotropic and nonhomogeneous. Variation of strength and other properties of the material depend on the orientation of load-to-direction of fiber reinforcement. This results in a significant modification of the conventional strength of material equations for reinforced sections.[3] Certain aspects relating to load orientation will be discussed in depth in the following chapter.

Advantages and Disadvantages of FRP

Among the advantages of this material are its resistance to corrosive atmosphere, high tensile strength and high strength-to-weight

ratios. Also beneficial are its excellent electrical properties, good machinability and pleasing appearance.[4] Some of the disadvantages and deterrents to its use include its low modulus of elasticity, brittleness, its unknown creep, plastic flow and fatigue characteristics. What is detrimental from the engineer's point of view, however, is the lack of standards in the plastics industry for structural design. This is mostly due to the lack of suitable design criteria.

Plastics in Construction Today

The significance of reinforced plastics as the construction material of the future is readily apparent by examining its past growth. Within the last 20 years, the plastic industry has seen an increase in production of 1,300 per cent. Futhermore, within the past eight years the per capita usage has increased from 32.7 lbs. to 70 lbs.[4]

The construction industry is the most fertile, relatively untapped market for further application of fiberglass reinforced plastics. Currently, the use of plastics represents $500 million in contracts or one per cent of the total use by the three conventional building materials: concrete, steel and wood. This figure will increase sharply over the next ten years as the necessity for pre-panelized partial and complete building packages will be realized because of the skyrocketing construction and erection costs.[4]

Summary of Literature Researched

At this time the most comprehensive studies of reinforced plastics are found in the following references: Engineering Design for Plastics edited by Eric Baer[2], a handbook prepared by Syracuse University

for the United States Air Force[5], and "Fiberglass Reinforced Plastics" by Ralph H. Sonneborn.[6]

The book edited by Eric Baer devotes an entire chapter to reinforced plastics using orthotropic plate theory. First, an analysis is given for the solution of the composite stresses in a parallel-filament laminate loaded in tension parallel to the filaments. These stress expressions are used in deriving approximate values for the laminate elastic constants in the principal material directions. The analysis is extended to include the evaluation of the material modulus and shear strain for an orthotropic plate loaded with biaxial normal stress and shear stress in directions different from the principal material directions. This procedure has appeared several times in the literature.[5,6] Design considerations for composite laminates are not included in this text.

Certain design aspects of composite laminates are discussed, however, in the United States Air Force Handbook. The most pertinent subject mentioned is design for tensile loads. An analysis is given for a member composed of more than one laminate bonded together in a composite in such a way that one set of laminates have their properties orientated in one direction, and a second set in another direction. When axial loads are applied to the composite, the analysis shows how stresses in each laminate layer can be evaluated. This approach assumes that the properties of the composites are known in the direction of load. The description of the design problem is very brief and is written in such a way that it is of little practical use to a civil engineer.

Ralph H. Sonneborn's book contains valuable information regarding the assumptions that must be made in designing with frp. (Part of these assumptions were used in Chapter II of this thesis in developing the flexure and deflection equations). Design examples are given, but they deal only with orthotropic plates subject to tensile loads. There is also a section that discusses computation of bending stresses in an isotropic composite beam. This, however, cannot be applied to the type of frp beam used in this thesis since it has non-isotropic properties.

In conclusion then, it can be stated that most current publications cover principally fiberglass reinforced plastics subject to tensile loads only. Design for flexure, deflections, shear, load combinations, load duration, short-time impact and creep have not at this time been developed. The following chapter of this study introduces a design theory for calculations of beam stresses and deflections on fiberglass reinforced plastics. An experimental study to verify the theory is presented in Chapter III.

CHAPTER II

FLEXURE AND DEFLECTION THEORY FOR FRP

To develop a design theory for fiberglass reinforced plastics, certain important assumptions must be made. The most basic one is that the strains in the fiber and resin are equal; in other words, the elongation and compression of fibers and of the resin are equal.[6] This assumption implies that a good bond exists between the fiber and resin, either inherently or because of the surface treatment of the glass, for mechanical interlock. It should be noted here that due to fabrication variables, an absolutely continuous bond may not exist.[7] However, if the bonded points are spaced close enough to develop a combined reinforcing action, then a satisfactory equivalent bond will exist. Furthermore, this bond, whether intermittent or continuous, must prevent any slippage between reinforcement and matrix. It must also prevent any buckling of the reinforcement.[6]

The second major assumption is that the composite material is linearly elastic; that is, the material obeys Hooke's Law. Hence the strains are directly proportional to the applied stresses. This assumption is a close approximation of what actually occurs under an uniaxial stress condition below the proportional limit. However, when frp is subjected to higher stresses, the second assumption breaks down. This occurs because the material may experience a plastic flow condition, especially in the matrix, resulting in substantial creep. To include

creep data as part of the design presents numerous problems. The first is that creep is a time-dependent deformation. A cartesian plot of strain versus time demonstrates this behavior, but it is of little use in describing creep over long time intervals. Because creep is non-linear, it is therefore difficult to handle graphically and mathematically. Futher complicating the design is the fact that creep involves a number of other interacting variables (e.g. temperature and stress) which require complex organization and presentation of data.[8] Thus the validity of the second assumption is open to question for long time loading, but it is reasonably accurate for short time loading.

The third assumption that was made in developing a design theory was that the fibers were unstressed in their state prior to loading. The following sections attempt only to set forth the design theory for stresses and deflections due to bending alone in a fiberglass reinforced plastic beam. Time did not permit other investigations. As more design data becomes available for these materials, the design procedures may be modified to include the combined effects of flexure, shear and torsion.

The Stress Equation

The type of reinforcing used in the development of this theory was the woven cloth variety with reinforcing rovings of equal area in two principal directions (Figure 1). These directions, longitudinal (warp) and transverse (fill) are at right angles to each other. The composite structure is called orthotropic or aelotropic.

A typical reinforced fiberglass beam is shown in Figure 2. It is essentially a multilayered beam with layers of rovings laid up parallel

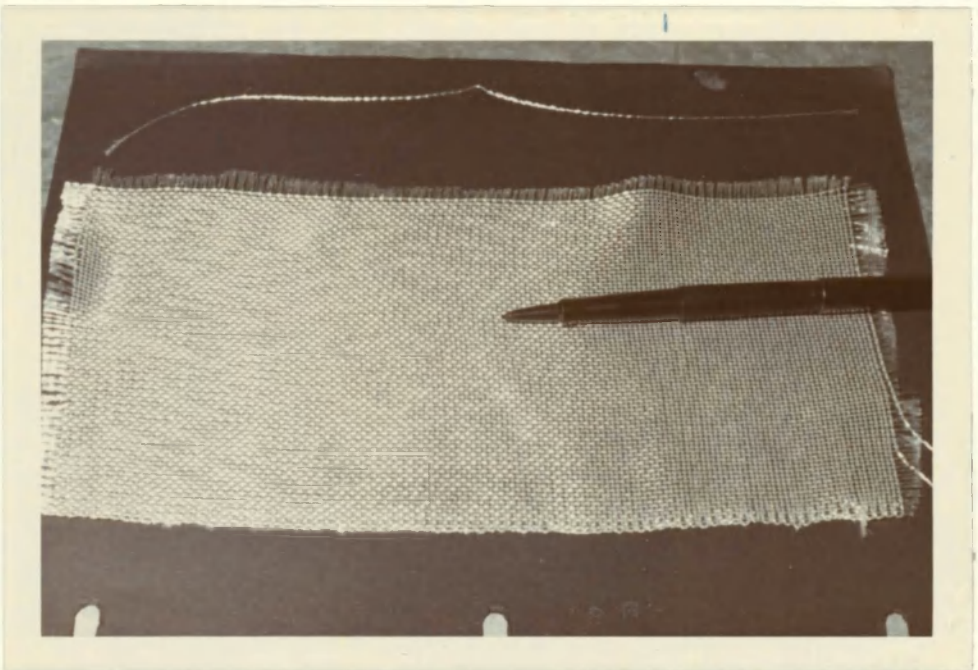

Figure 1. Typical Glass Woven Roving Cloth

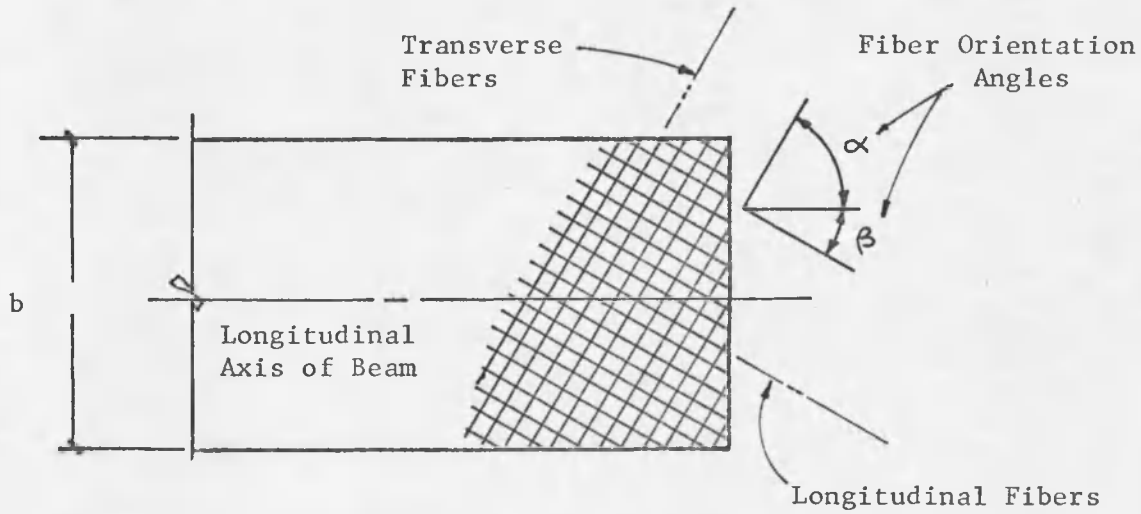

Plan

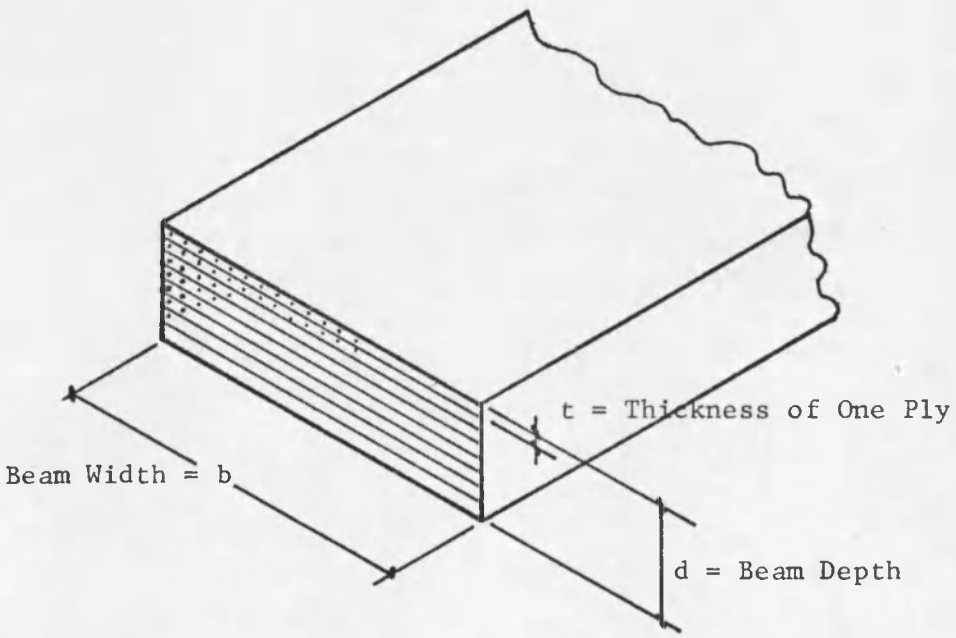

Isometric

Figure 2. Terminology for FRP Beams

to each other and bonded together by the matrix to form the composite section.

Consider now such a composite beam subjected to pure bending with a distribution of internal forces as shown in Figure 3. Futhermore, let this force distribution be made up of incremental P forces. Therefore, if one of these P forces is examined in plan, a distribution of force components between the fiber and matrix can be obtained (Figure 4).

To arrive at an expression for the fiber and matrix stresses, the first step will be to sum forces. Referring to Figure 4, the summation of forces in the Y' direction will yield

$$\sum F_{y'} = 0 = A_f s_f \sin\alpha - A_f s_f' \sin\beta \qquad \text{.....(1)}$$

Using the relationship $\beta = 90^\circ - \alpha$, (1) can be rewritten as

$$\sum F_{y'} = 0 = A_f s_f \sin\alpha - A_f s_f' \cos\alpha \qquad \text{.....(2)}$$

From (2), a relation between the fiber stresses in the longitudinal and transverse directions can be obtained. The expression becomes

$$\frac{s_f'}{s_f} = \frac{\sin\alpha}{\cos\alpha} \quad \text{or} \quad \frac{s_f'}{s_f} = \tan\alpha \qquad \text{.....(3)}$$

Summing forces and components along the X' axis gives

$$\sum F_{x'} = 0 = -P_y + A_f s_f \cos\alpha + A_f s_f' \cos\beta + A_m s_m \qquad \text{.....(4)}$$

To get the true representation of the fiber areas acting normal to the component loads, the angle orientation of the fiber must be taken into

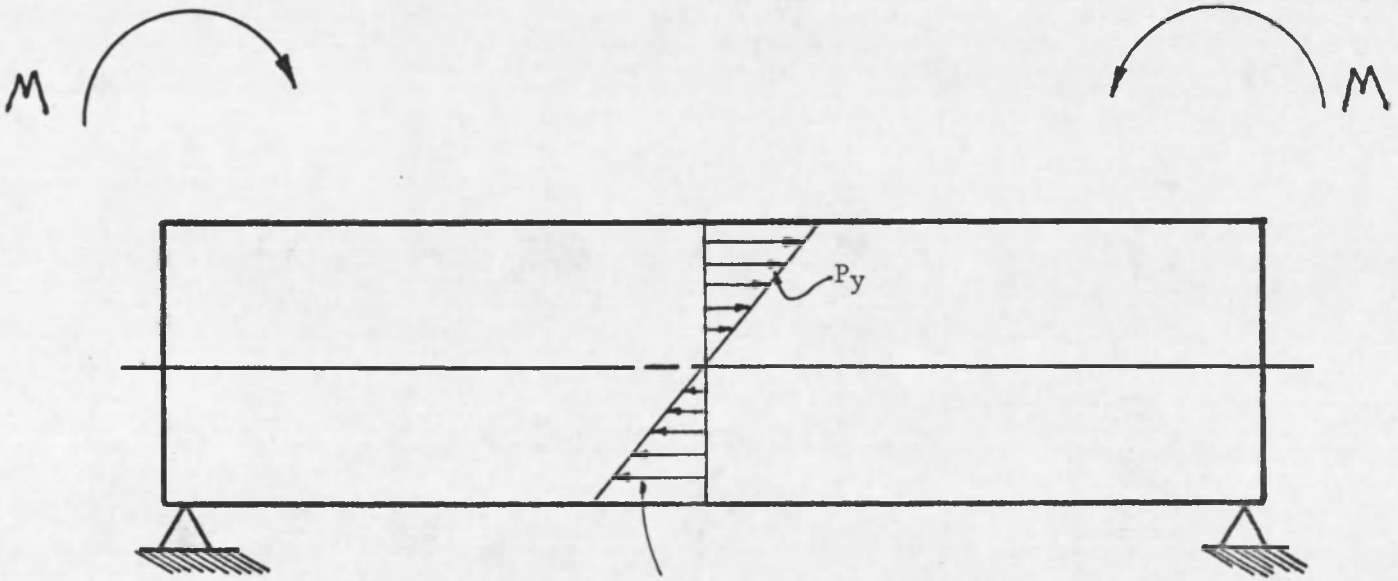

Figure 3. Beam Subject to Pure Bending

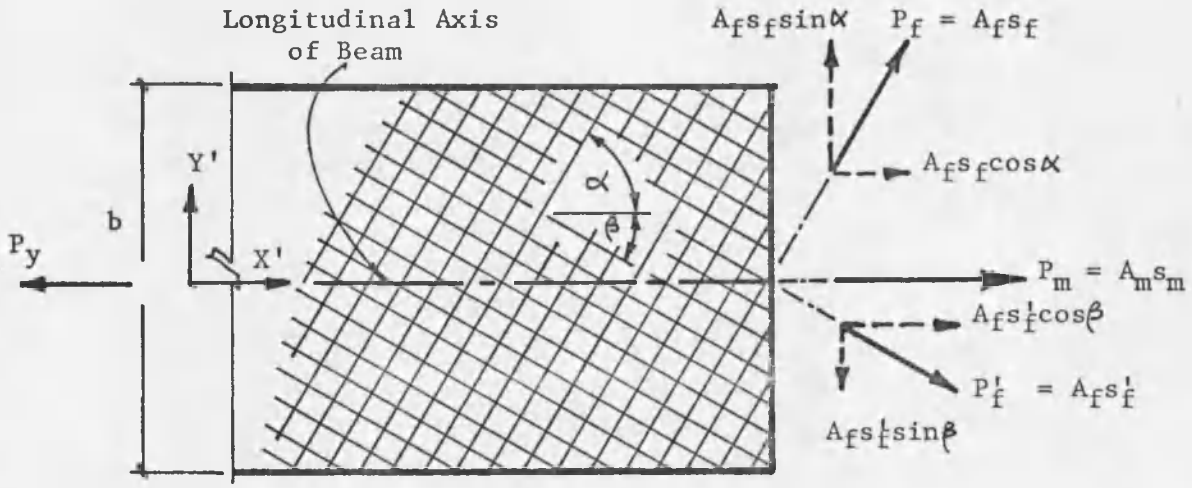

where: b = Beam Width

α = Orientation of Transverse Fibers With Respect to the Longitudinal Axis of Beam

β = Orientation of Longitudinal Fibers With Respect to the Longitudinal Axis of Beam

s_m = Matrix Stress

s_f = Fiber Stress in Transverse Fibers

s_f' = Fiber Stress in Longitudinal Fibers

P_f = Force Component in Transverse Fibers

P_f' = Force Component in Longitudinal Fibers

P_y = Resultant Force Acting at a Distance y From the Neutral Axis in X direction

P_m = Force Component in Matrix

A_m = Net Cross-Sectional Area of Matrix in One Ply Thickness

A_f = Total Cross-Sectional Area of Fibers in One Ply Thickness Acting in Transverse or Longitudinal Direction

Figure 4. Force Diagram

account. Referring to Figure 5, the component of area acting normal to the force $A_f s_f \cos\alpha$ would be

$$\frac{A_f}{\cos\alpha}$$

Similarly the component of area acting normal to the force $A_f s_f' \cos\beta$ is

$$\frac{A_f}{\sin\alpha}$$

Let us define A_m as the net cross sectional matrix area in one ply; therefore the following expression can be written

$$A_m = bt - \frac{A_f}{\cos\alpha} - \frac{A_f}{\sin\alpha}$$

Equation (4) can now be more conveniently rewritten as

$$P_y = A_f s_f \cos\alpha + A_f s_f \tan\alpha \sin\alpha + \left[bt - \frac{A_f}{\cos\alpha} - \frac{A_f}{\sin\alpha} \right] s_m \quad \ldots\ldots\ldots (5)$$

In order to find a solution for equation (5), a second expression involving s_f and s_m must be derived. This can be done using the assumption that the X components of strain in the fiber and matrix are equal. In Figure 6, the following relationships are shown

$$E_m = \frac{s_m}{\frac{\epsilon_m}{1}} \quad \text{and} \quad E_f = \frac{s_f}{\frac{\epsilon_m \cos\alpha}{\frac{1}{\cos\alpha}}}$$

where E_m and E_f are the Moduli of Elasticity for the matrix and fiber.

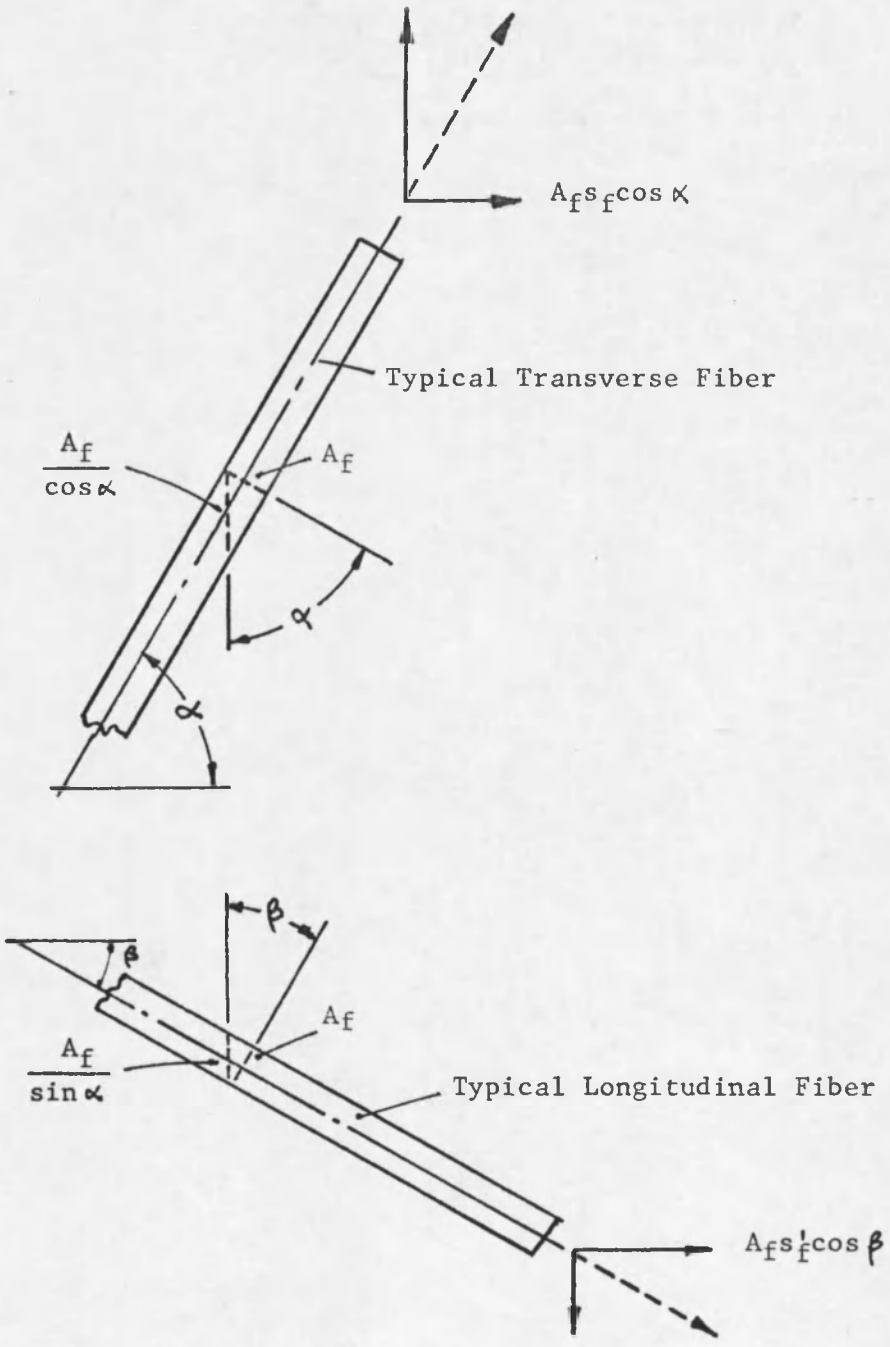

Figure 5. Orientation of Glass Fibers

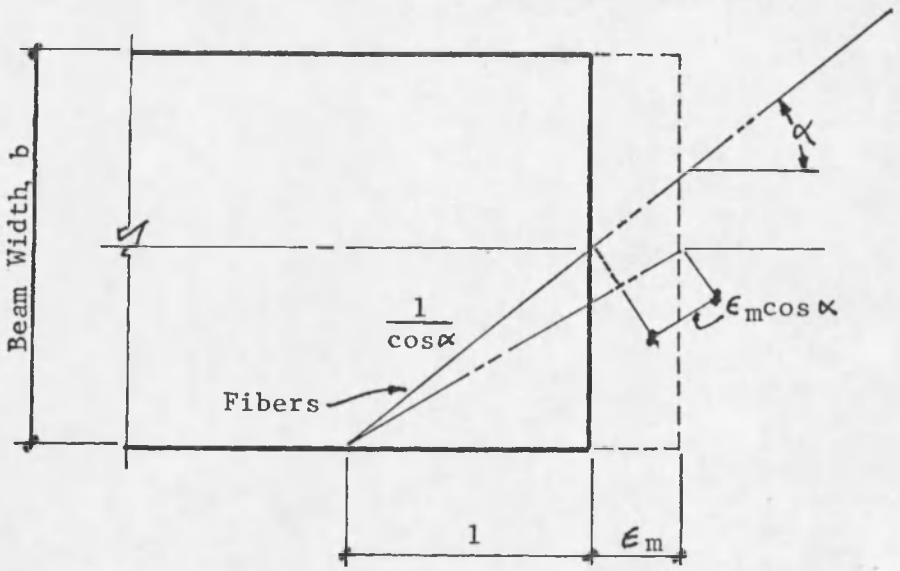

Figure 6. Deformation Diagram

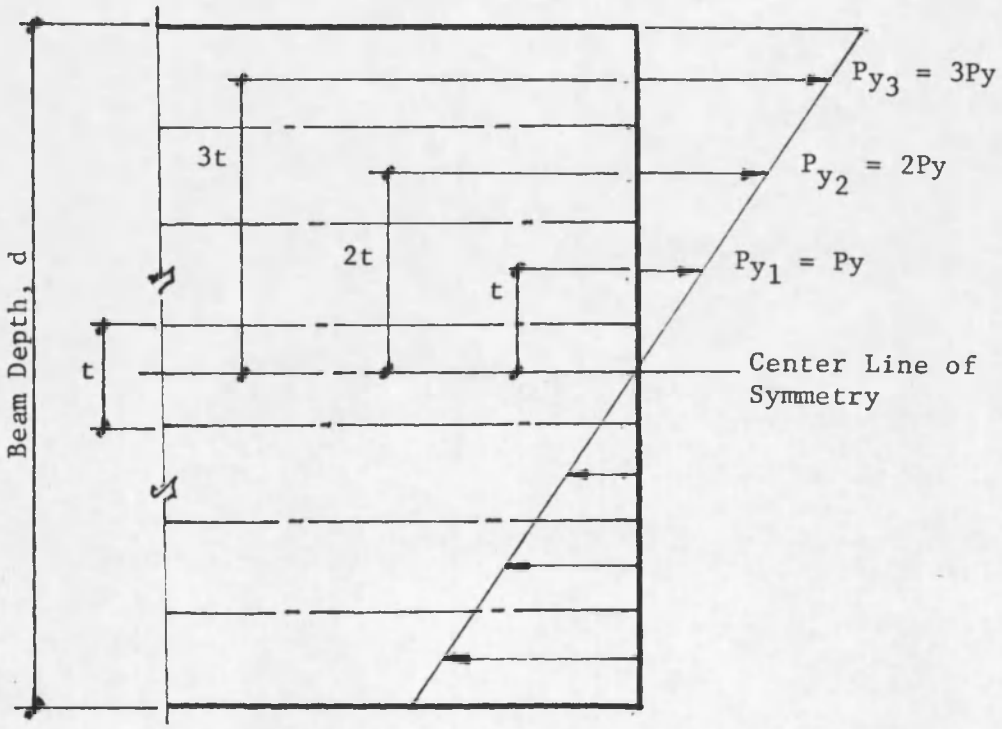

Figure 7. Distribution of Forces

This can be simplified to give

$$E_m = \frac{s_m}{\epsilon_m} \quad \text{and} \quad E_f = \frac{s_f}{\epsilon_m \cos^2\alpha}$$

Here ϵ_m represents the strain in the matrix, while $\epsilon_m \cos^2\alpha$ represents a compatible strain in the fiber. Solving these expressions for ϵ_m, the following relationships are obtained

$$\frac{s_m}{E_m} = \frac{s_f}{E_f \cos^2\alpha} \qquad \text{.....(6)}$$

Solving equation (6) for s_m and substituting this value into equation (5) yields

$$P_y = A_f s_f \cos\alpha + A_f s_f \tan\alpha \sin\alpha + \left(bt - \frac{A_f}{\cos\alpha} - \frac{A_f}{\sin\alpha}\right) x \ldots$$

$$\ldots x \left(\frac{s_f E_m}{\cos^2\alpha E_f}\right) \qquad \text{.....(7)}$$

Equation (7) represents the value of a force P acting at a distance y from the neutral axis of the beam. If a seven ply beam is used as an example (Figure 7), and the distance to each P force is represented by the ply thickness t, then the summation of moments about the neutral axis results in the expression

$$M = 2 \left[P_y t + 2P_y(2t) + 3P_y(3t)\right]$$ (neglecting small contribution of middle ply).

The general expression for the moment in the beam could thus be written as

$$M = \sum_{k=3,5,7\ldots}^{n} \left(\frac{k-1}{2}\right)^2 2P_y t \qquad \ldots\ldots\ldots\ldots (8)$$

where n is the total number of plys in the beam depth. Substituting equation (7) into equation (8) gives the final equation of moment involving only one unknown, s_f.

$$M = \sum_{k=3,5,7\ldots}^{n} \left(\frac{k-1}{2}\right)^2 2t\left[A_f s_f(\cos\alpha + \tan\alpha\sin\alpha) + \left(bt - \frac{A_f}{\cos\alpha} - \frac{A_f}{\sin\alpha}\right)\left(\frac{s_f E_m}{\cos^2\alpha E_f}\right)\right] \quad ..(9)$$

It should be noted that s_f is the fiber stress at a distance t from the neutral axis of the beam. It is not the outermost fiber stress. Furthermore, equation (9) is valid only so long as the allowable matrix stress is not exceeded.

The Deflection Equation

Although the effect of creep upon the deformation of the material is an important consideration for long time deformation, it would necessitate a long time testing program for creep data. The author will, therefore, restrict the development of a deflection equation for the subject of this thesis to that of short time loading of a cantilevered beam.

Figure 8 shows two fibers from an frp beam orientated at an angle of α and β with respect to the longitudinal axis of the beam. As was derived previously in equation (9), the force component in the fibers is

$$F = A_f s_f(\cos\alpha + \tan\alpha\sin\alpha)$$

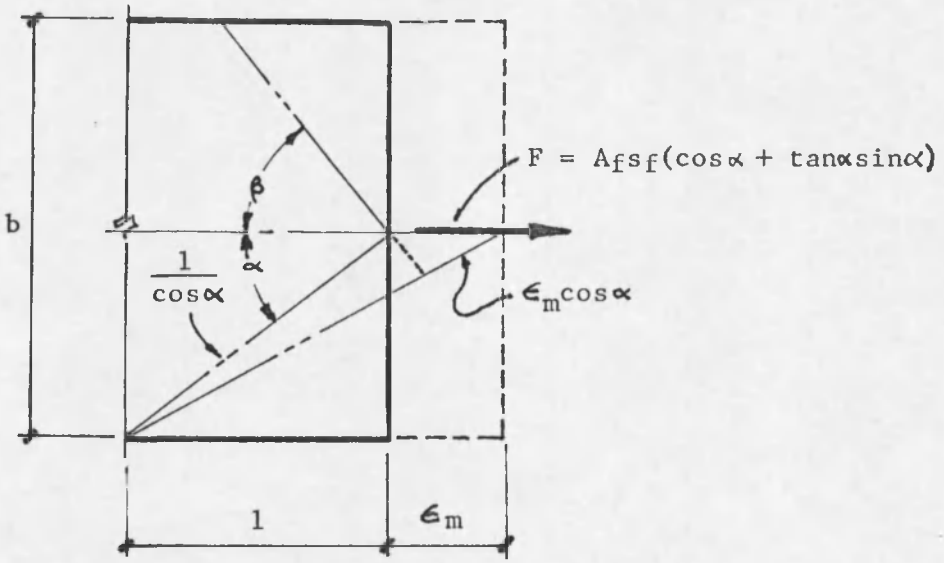

Figure 8. Fiber Force Resulting in Deformation

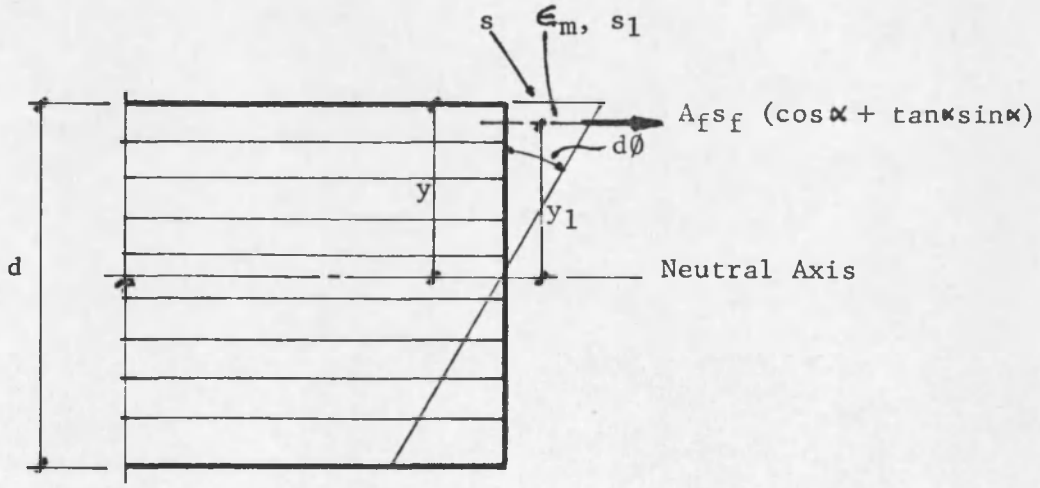

where: s = Outer Fiber Stress

s_1 = Fiber Stress at Level 1

Figure 9. Stress Distributions

Referring to Figure 9, the moment at the neutral axis of the beam could be represented by

$$M_x = \sum_{-y_n}^{y_n} yA_f s_f(\cos\alpha + \tan\alpha\sin\alpha) \qquad \text{.....(10)}$$

Furthermore by using similar triangles, the following relationship can be written

$$\frac{s_1}{y_1} = \frac{s}{y} \quad \text{or} \quad s = \frac{s_1 y}{y_1} \qquad \text{.....(11)}$$

Substituting this value of fiber stress into equation (10) gives

$$M_x = \frac{s_1}{y_1}(\cos\alpha + \tan\alpha\sin\alpha)\sum_{-y_n}^{y_n} y^2 A_f \qquad \text{.....(12)}$$

The quantity $\sum y^2 A_f$ represents an effective moment of inertia I for the fibers about the neutral axis. Therefore equation (12) can be simplified to obtain

$$M_x = \frac{s_1}{y_1}(\cos\alpha + \tan\alpha\sin\alpha)I_f \quad \text{where } I_f = \sum_{-y_n}^{y_n} y^2 A_f \qquad \text{.....(13)}$$

Also according to Figure 9, the following angular expression exists

$$d\phi = \frac{\epsilon_m}{y_1} \qquad \text{.....(14)}$$

Furthermore in Figure 8 it can be observed that

$$\epsilon_{\alpha f} = \epsilon_m \cos^2\alpha$$

where $\epsilon_{\alpha f}$ is the fiber strain in the α direction. Since

$$\epsilon_{\alpha f} = \frac{s_f}{E_f}$$

we can state that

$$\epsilon_m = \frac{\epsilon_{\alpha f}}{\cos^2 \alpha} = \frac{s_f}{E_f \cos^2 \alpha}$$

Substituting this final value of ϵ_m into equation (14) yields

$$d\phi = \frac{s_f}{E_f \cos^2 \alpha y_1} \qquad \text{where } s_f = s_1 \text{ at level 1}$$

so that

$$\frac{M_x}{d\phi} = \frac{s_1}{y_1} (\cos\alpha + \tan\alpha \sin\alpha) \frac{I_f E_f \cos^2 \alpha y_1}{s_1} \qquad \text{or}$$

$$\frac{M_x}{d\phi} = (\cos\alpha + \tan\alpha \sin\alpha) \cos^2 \alpha \, I_f E_f \qquad \text{and}$$

$$d\phi = \frac{M_x}{(\cos\alpha + \tan\alpha \sin\alpha) \cos^2 \alpha \, I_f E_f} \qquad \text{but since } M_x = Px \text{ (cantilevered end load)}$$

$$d\phi = \frac{Px}{(\cos\alpha + \tan\alpha \sin\alpha) \cos^2 \alpha \, I_f E_f} \qquad \text{and since } \triangle = \int_0^L d\phi x$$

the resultant deflection of the fibers can be written as

$$\triangle_f = \int_0^L \frac{Px^2}{(\cos\alpha + \tan\alpha \sin\alpha) \cos^2 \alpha I_f E_f} \qquad \text{or}$$

$$\Delta_f = \frac{PL^3}{3(\cos\alpha + \tan\alpha\sin\alpha)\cos^2\alpha\, I_f E_f} \qquad \text{.....(15)}$$

To obtain the deflection of the matrix, consider the matrix acting as a homogeneous material. The maximum matrix deflection for a cantilevered beam is given by

$$\Delta_m = \frac{PL^3}{3E_m I_m} \qquad \text{.....(16)}^9$$

The reciprocal of the deflection of a composite beam can furthermore be represented by

$$\frac{1}{\Delta} = \frac{E_1 I_1}{KML^2} + \frac{E_2 I_2}{KML^2} \qquad \text{.....(17)}^{10}$$

where M is the total moment taken by the beam; L is the length of the beam; E_1 and E_2 are the respective Elastic Moduli of the materials; and I_1 and I_2 are the respective moments of inertia. The term K represents a constant depending upon the condition of loading. Substituting the appropriate terms from equations (15) and (16) into equation (17), yields the reciprocal of the resultant deflection for a cantilevered beam loaded at the end,

$$\frac{1}{\Delta_t} = \frac{3E_m I_m}{PL^3} + \frac{3(\cos\alpha + \tan\alpha\sin\alpha)\cos^2\alpha\, I_f E_f}{PL^3} \qquad \text{.....(18)}$$

where $I_m = \frac{bd^3}{12} - I_f$,

$$I_{f'} = \sum_{-y_n}^{y_n} \frac{2A_f y^2}{\cos \alpha}$$

y = distance from neutral axis to centerline of fiber

$\frac{1}{\Delta t}$ = the reciprocal of the deflection for a cantilevered frp beam (maximum end deflection).

CHAPTER III

NATURE AND SCOPE OF TESTING

The previous chapter discussed the derivation of a stress and a deflection equation. To verify these theoretical expressions, the following testing procedure was planned:

1. A tension test would be conducted on both a single roving of glass fiber and on a bar of resin. From these tests, the respective Moduli of Elasticity could be determined for each of the materials.
2. A cantilevered frp beam would be loaded with a concentrated load at the free end, and the matrix strains measured.
3. Having obtained the values of E_m, E_f, ϵ_m, equation (9) could therefore be solved for the theoretical moment. This answer would then be compared with the actual bending moment.
4. The maximum deflections would be measured at the point of loading and these results would be compared to the theoretical results by using equation (18).

Description of Test Specimens and Materials Used

In equation (9), the elastic constants E_f and E_m are employed. Rather than rely on approximations for these values, tension tests were made on glass roving and polyester resin specimens to determine each Modulus of Elasticity. Having obtained the data, the matrix strain could

be measured from an frp beam specimen. The exact value of equation (9) could thus be obtained.

Glass Fiber Specimen

One roving fiber was removed from a fibrous mat (Figure 1) for tension testing. This roving was made up of numerous individual strands composed of Pittsburg Plate Glass (6oz. cloth No. 58502) having a total net area of .000208 square inches per roving. Each end of the roving was embedded in a resin block (Figure 10) to provide a gripping surface for the tension test apparatus.

Composition and Manufacture of Fibers. As with other forms of glass, the basic ingredient of glass fiber is silica or silicon dioxide (SiO_2), which in the pure state is colorless to white. To manufacture the basic fiber, silica is mixed with lime, alumina, and boron trioxide. It is then fed into a furnace where it is heated to the molten state. The batch of molten glass is then rolled into small marbles which are fed into spinnerettes. From here the molten glass is drawn into the final glass filament and bundled to form roving.[3]

Resin Specimen

The resin used throughout this experimental study was a polyester thermosetting resin. Thermosetting materials are those that undergo a chemical polymerization reaction when heated. Reheating does not reverse the process.[6] The approximate dimensions of the resin material used in the tension test are shown in Figure 11.

Characteristics of Polyester Resins. The resins may be formulated from a variety of alcohols, acids, and cross-linking monomers.

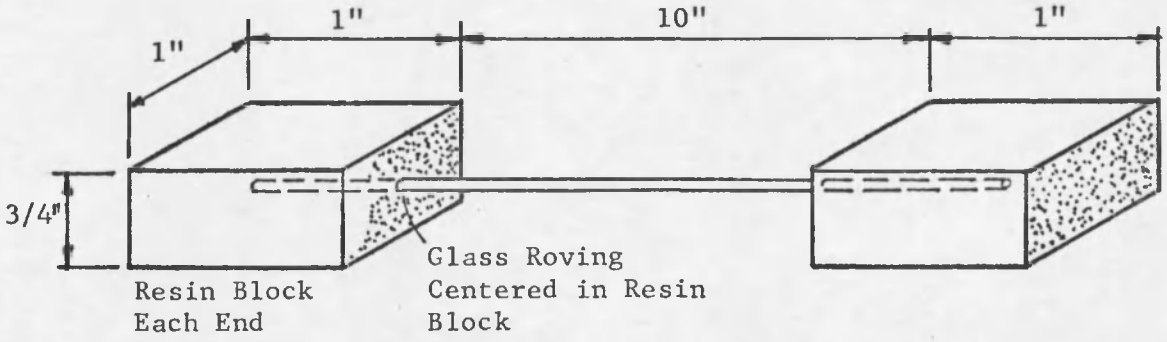

Figure 10. Fiber Tension Test Specimen

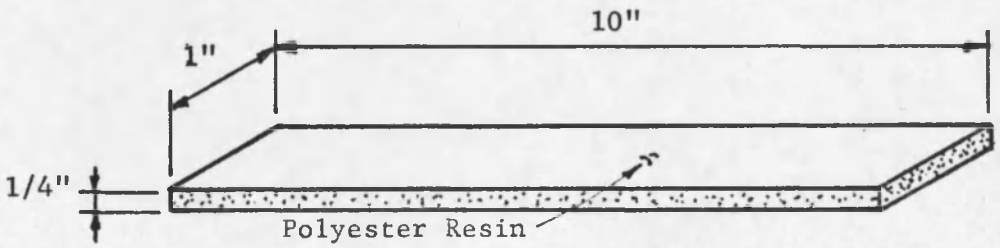

Figure 11. Resin Tension Test Specimen

Therefore, they can take many forms: the most common being referred to as "general purpose polyesters." The following are some characteristics of this type:[6]

Color	water-white
Viscosity @ 75°F	600 to 2500 cp
Specific Gravity @ 75°F . .	1.1 to 1.2
Solubility	insoluble in water; soluble in ketones and a few other organics

Beam Specimen

Successive layers of reinforcing mat fibers and polyester resin were laid up to form the beam specimens as illustrated in Figure 12. Because of the length of time involved in securing one of these composite beams from the manufacturer, only three sample types were obtained. The variables introduced were the total ply thickness of the beam and the orientation of the mat fibers. The width and length dimensions, however, were kept constant for each test specimen.

Tension Test and Instrumentation

The testing apparatus was a Tinius-Olsen Universal Test Machine (Figure 13). For the glass fiber specimen, a dial indicator was used to measure the incremental change in length in computing the strain. In the case of the resin specimen, however, a clamp-on two inch mechanical strain indicator gave direction readings of strain in ten-thousands of an inch. In each of the tests preformed, the "low range" scale on the Tinius-Olsen was used to give increments of two pounds per dial division. Three test samples, each of resin and fiber, were used in the tension

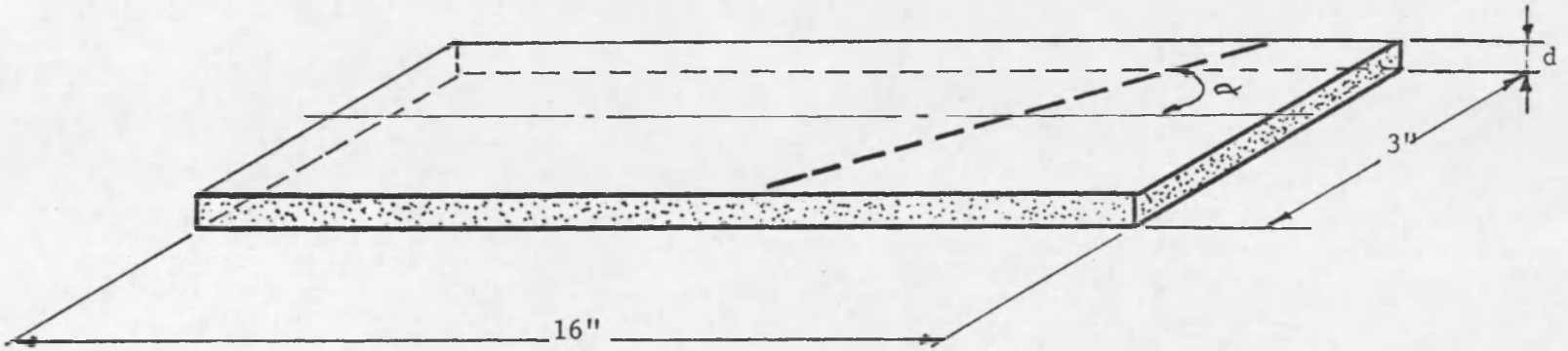

Specimen 1. d = .1025 in. (11 Ply)
$\alpha = 45^{o}$

Specimen 2. d = .250 in. (25 Ply)
$\alpha = 45^{o}$

Specimen 3. d = .250 in (25 Ply)
$\alpha = 30^{o}$

Figure 12. Typical FRP Beam Specimens

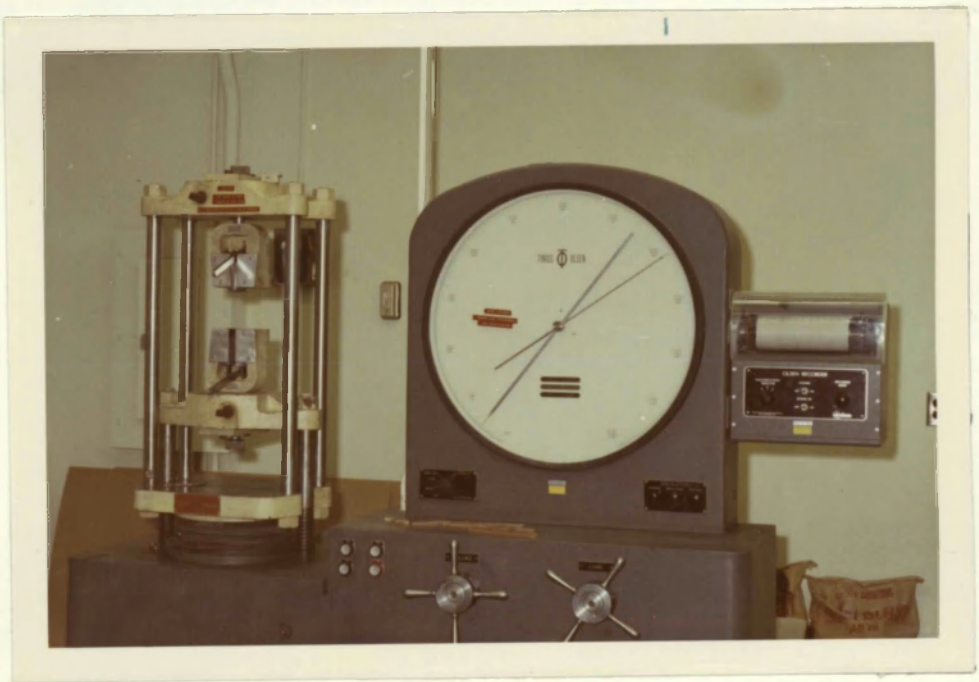

Figure 13. Tension Test Apparatus

tests. All testing was performed at room temperature. The following procedure was used for testing both materials:

1. The specimens were secured to the wedge-type clamping device furnished with the Tinius-Olsen apparatus.
2. The load and strain indicators were zeroed.
3. Load was applied at a uniform rate of approximately one pound per second, while strains were read at each one-hundred and two pound increments for the resins and glass fiber respectively.
4. Step (3) was continued until enough readings were made to plot a stress-strain curve.

Stress Test and Instrumentation

A typical test setup is shown in Figures 14 and 15. An frp beam was securely clamped at one end and subjected to various concentrated loads at the free end. By use of strain gages and indicator, the matrix strain at the outermost top fiber was measured. Throughout the testing, SR-4, 120-ohm paper strain gages were employed. These gages were bonded to the beam with a uniform coating of "Duco Cement" and allowed to set for 24 hours before conducting any testing.

The basic principle of operation of these strain gages is simple. When a load is applied to the beam, the outer fibers expand causing strain in the material. If a grid of wire is bonded to that object, it will stretch or be strained exactly as the surface of the test specimen. A reading of the strain can be calibrated electronically when an electric current is allowed to pass through the filament grid to an

Figure 14. Strain Test Apparatus

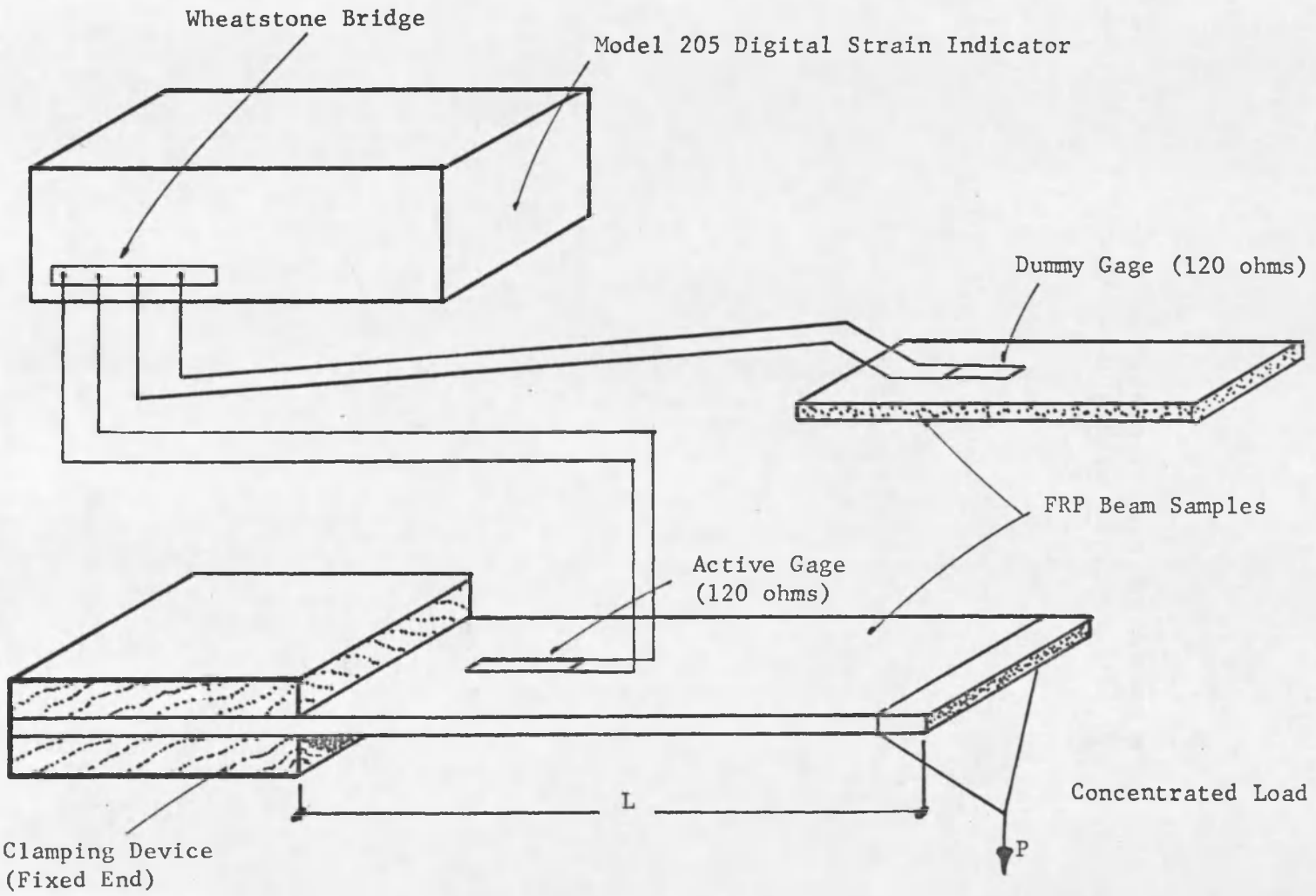

Figure 15. Schematic of Strain Test

appropriate indicator. The change in resistance of the stretched gage wire is proportional to the strain on the surface of the test member.

The simple form of a Wheatstone Bridge used in the testing has one serious defect. The SR-4 gage used has filament wires that are temperature-sensitive as well as strain-sensitive. To cancel out any effect of temperature on the gage wire, a circuit like that shown in Figure 16 was used. This arrangement employs two gages as adjacent arms of the bridge. Therefore in this experiment, one of these, the "active" gage A, was mounted on the stressed material. The other, the "dummy" gage B, was attached to an unstressed piece of the same material. As shown in Figure 14, the two gages are located close together so that both are subjected to substantially the same temperature. In order to measure the distribution of strain across the width of the beam, three gages were attached to the twenty-five ply specimens as shown in Figure 17. The eleven-ply specimen had one strain gage mounted in the center only (Figure 18).

The indicator used was the BEC-205 Digital Strain Indicator. It gives a direct readout of strain in microinches per inch from the environmental resistance changes of the strain gages. Digital readout is completely electronic with a luminous display of four digits plus polarity.

Deflection Measurements

Since the deflections obtained were relatively large, the simple apparatus shown in Figure 19 was used to give direct readings. An initial point was marked on the graph paper by a slight indentation of the

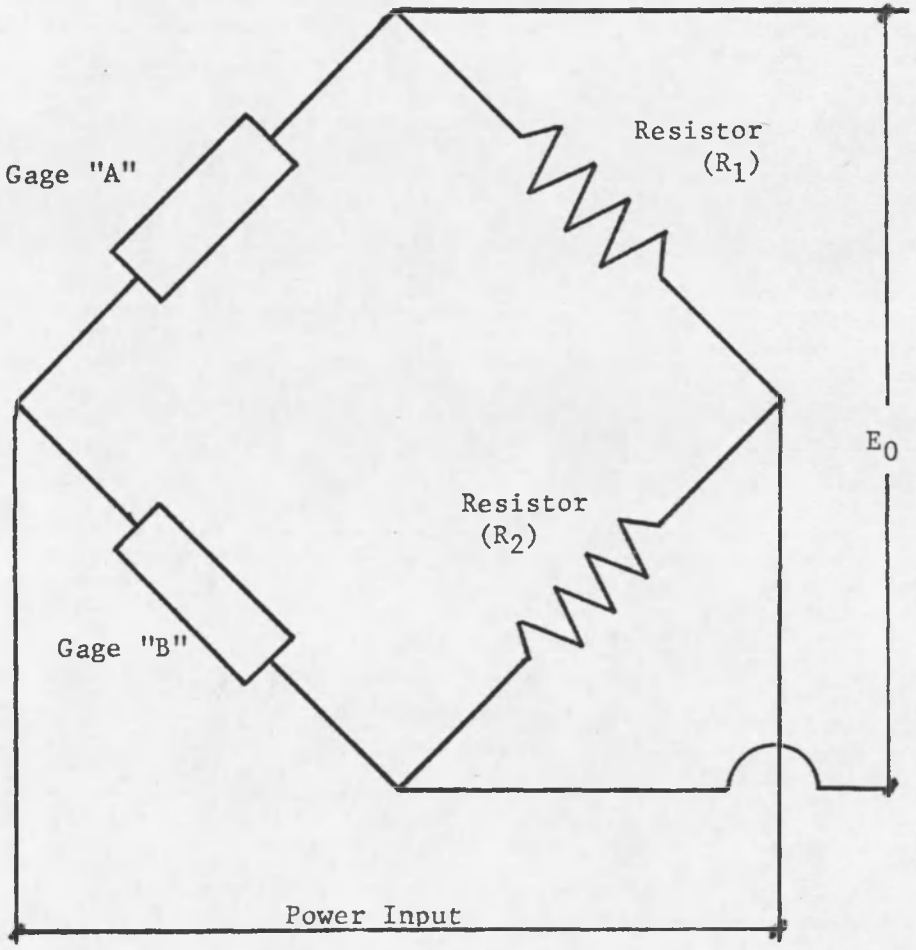

Figure 16. Bridge Circuit

Figure 17. Attachment of Gages to 25 Ply Beam

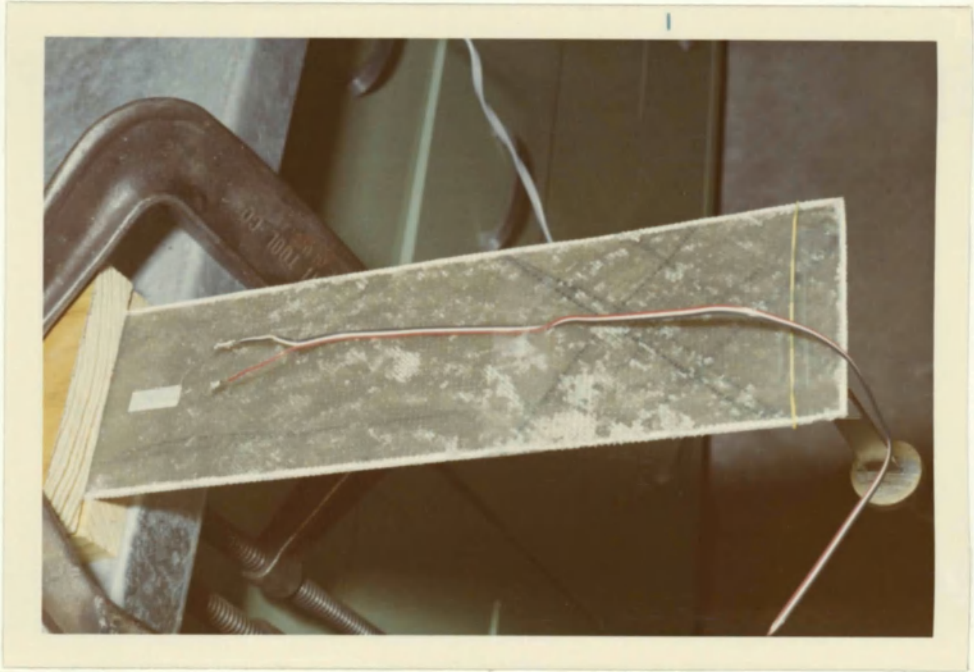

Figure 18. Attachment of Gage to 11 Ply Beam

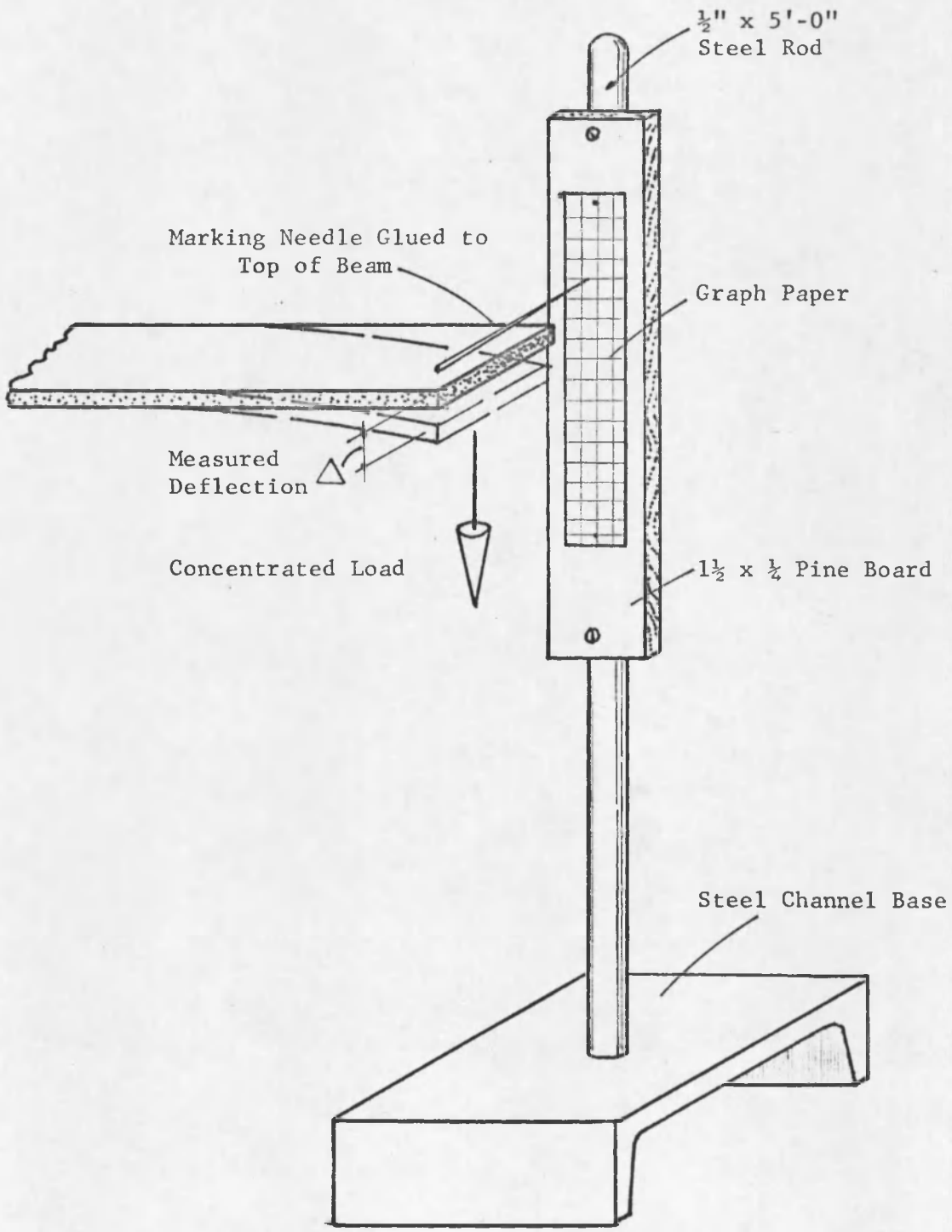

Figure 19. Deflection Measuring Apparatus

marking needle. After applying the load and allowing the beam to deflect to its maximum position, the final indentation was made. Three trail deflections were measured for each load applied. The actual deflections were measured from the indentation on the graph paper with a caliper. The deflections were measured on each side of the specimen to determine if there were any significant torsional strains.

CHAPTER IV

TEST RESULTS

Glass Fiber Tension Test Results

It was not possible to arrive at a test value for the Modulus of Elasticity of the glass roving because of bonding failures within the individual glass fibers. The fault was in the test procedure; that is, there was no matrix material surrounding the glass rovings to provide for the continuity needed. When the glass rovings act in tension as part of a fiberglass reinforced beam, they are prevented from fraying by the resin matrix. Thus, the integrity of the glass roving is not affected. However, without this matrix, as in the case of the tension test, the glass fibers lack continuity and hence fail at much lower stress levels. Therefore, due to a lack of test data, an approximation of 7,000,000 psi was used as the Modulus of Elasticity for the glass.[2] Figure 20 shows a typical tension failure (note the frayed ends of the glass fiber).

Resin Tension Test Results

Figure 21 shows the stress-strain curves derived for the three specimens tested. It should be noted that it required approximately 200 pounds of tensile force before any data was obtained. It was expected that this would occur since there was an initial period when some slippage and set occured at the time the load was first applied. The three resin specimens experienced a brittle fracture at a load of 1300 to 1400

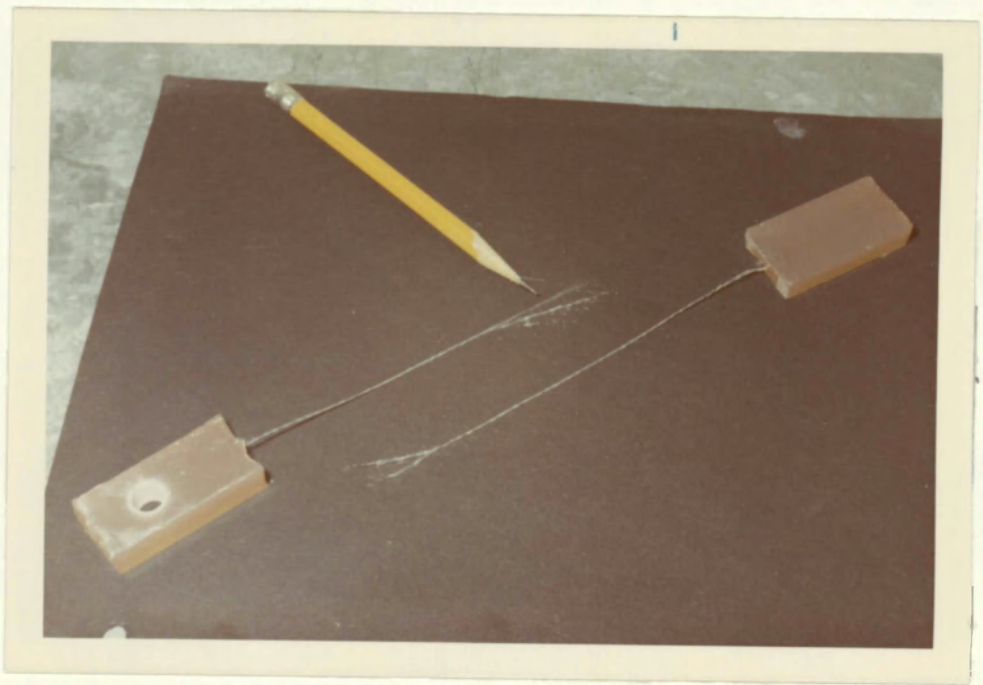

Figure 20. Typical Tensile Failure - Glass Fiber

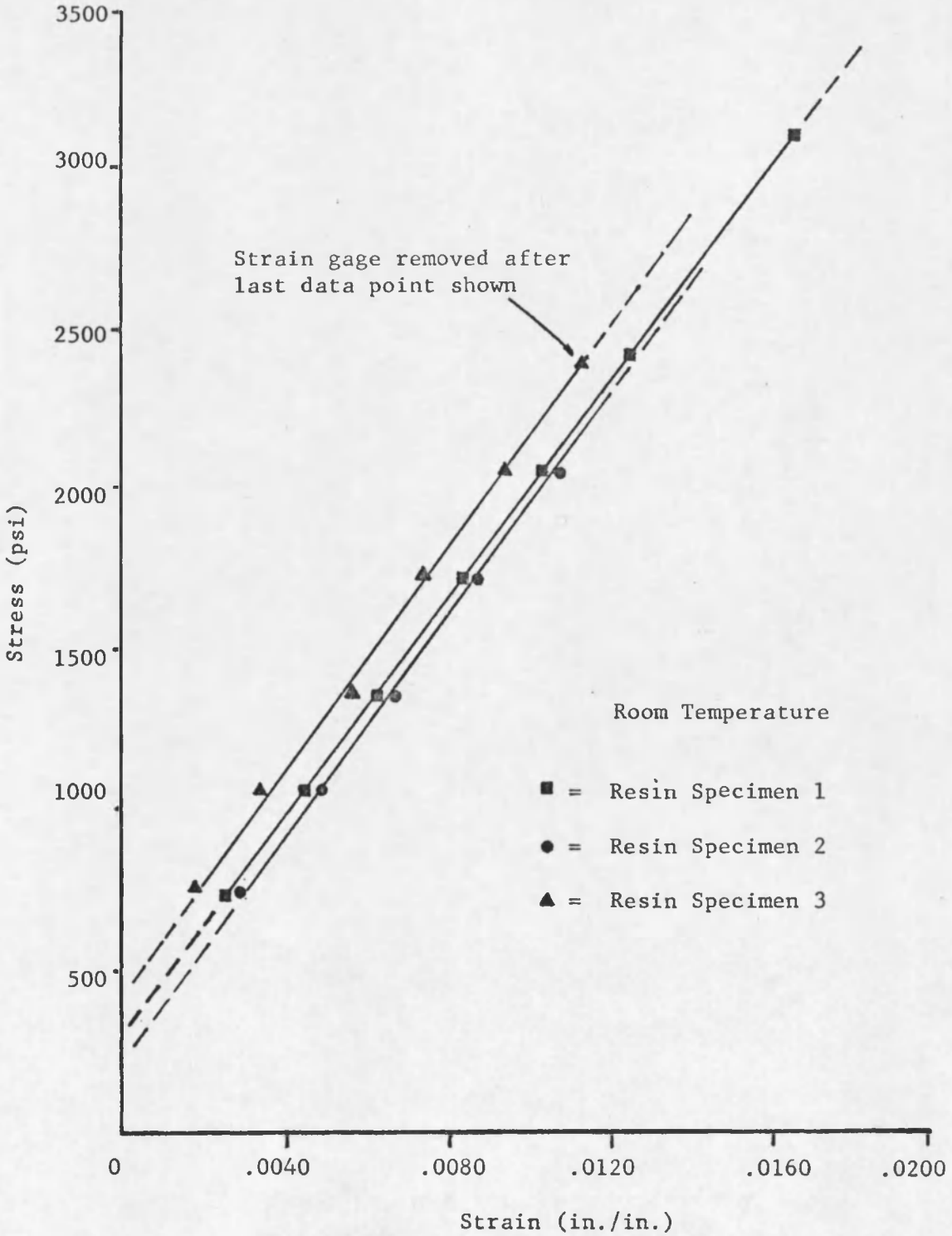

Figure 21. Stress-Strain Curves - Resin

pounds (Figure 22). Since the cross-sectional areas of the specimens were .290 in.^{2}, the resulting maximum tensile strength was

$$s_{max} = \frac{1400}{.290} = 4800 \text{ psi}$$

This value of stress does not appear in Figure 21 since the strain gage was removed prior to failure of the specimen. The maximum tensile strength could have been increased somewhat if the resin specimen was vibrated during its "setting time"; that is, vibration could have eliminated some of the air bubbles and increased the tensile strength.

Referring to Figure 21, the resin's Modulus of Elasticity was calculated as follows:

$$E_1 = \frac{2420 - 692}{.0125 - .0024} = \frac{1728}{} = 171{,}000 \text{ psi}$$

$$E_2 = \frac{1730 - 692}{.0083 - .0024} = \frac{1038}{.0059} = 175{,}000 \text{ psi}$$

$$E_3 = \frac{2080 - 692}{.0102 - .0024} = \frac{}{.0078} = 177{,}000 \text{ psi}$$

Therefore, the average Modulus of Elasticity was $E_m = 174{,}000$ psi.

Stress and Deflection Test Results

Tables I, II, and III show the correlation of test data and the theoretical analysis as computed by equations (9) and (18). The combined results of the three test specimens showed that there was a 6% average error for the stress equation and a 4% average error for the deflection equation. These small departures may have been due to inaccurate fabrication of the beams and a lack of uniform distribution of

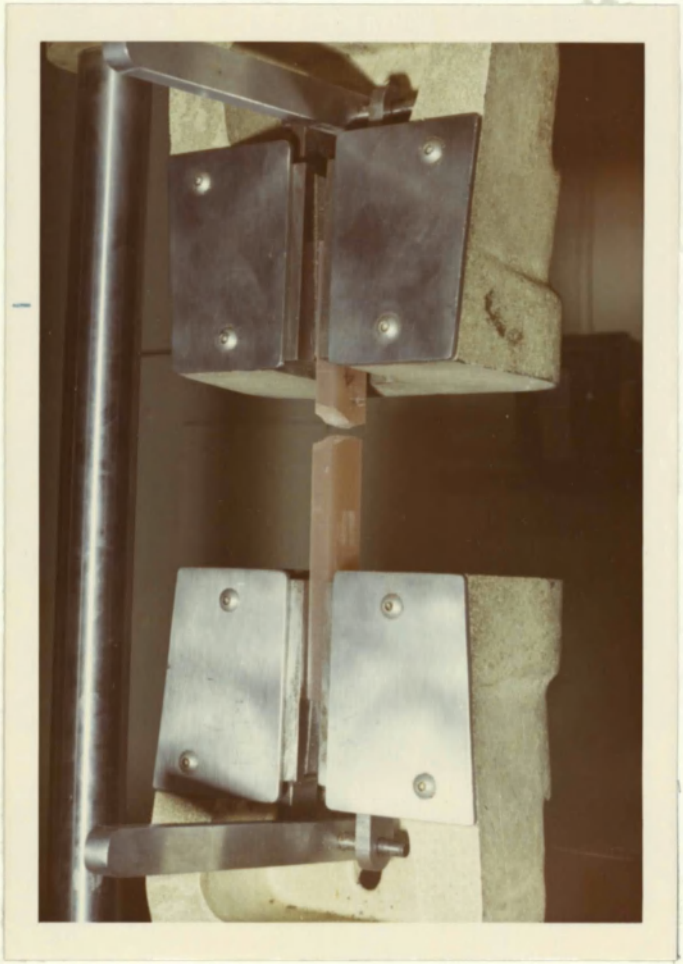

Figure 22. Typical Tensile Failure - Resin

Table I. Stress and Deflection Results - Specimen No. 1

P	ϵ''_m	s''_m	s_m	s_f	Eq.(9) M	M_a	% Error	Δ_a	$1/\Delta_a$	Eq.(18) $1/\Delta_a$	% Error
lbs.	$\frac{\mu in.}{in.}$	psi	psi	psi	in.-lb.	in.-lb.	-	in.	1/in.	1/in.	-
.066	94	16.4	2.96	59.5	.63	.59	4.0	.072	13.90	13.90	.000
.132	183	31.8	5.80	117.0	1.28	1.19	6.6	.145	6.90	6.95	.725
.200	270	47.0	8.55	173.0	1.86	1.80	3.0	.218	4.60	4.59	.222
.266	362	63.0	11.50	232.0	2.56	2.40	7.5	.288	3.48	3.46	.575
.330	450	78.2	14.20	286.0	3.09	2.97	6.8	.357	2.80	2.79	.358

Error Average 5.6% Error Average .376%

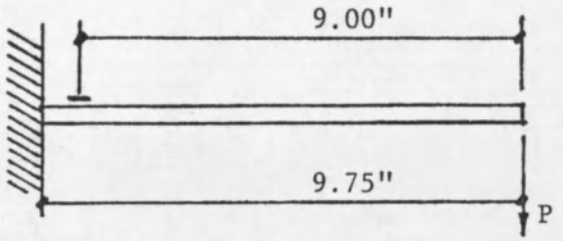

Data: $\alpha = 45^{o}$

$d = .1025$ in.

$b = 3.000$ in.

$A_f = .0075$ in.^{2}

Table II. Stress and Deflection Results - Specimen No. 2

P	ϵ''_m	s''_m	s_m	s_f	Eq.(9) M	M_a	% Error	Δ_a	$1/\Delta_a$	Eq.(18) $1/\Delta_a$	% Error
lbs.	$\frac{\mu in.}{in.}$	psi	psi	psi	in.-lb.	in.-lb.	-	in.	1/in.	1/in.	-
.33	87	15.1	1.21	24.6	3.50	3.46	1.50	.055	18.00	17.80	1.1
.60	157	27.3	2.18	44.2	6.31	6.25	.97	.100	10.00	9.94	.6
1.03	280	48.6	3.90	79.0	11.30	10.80	4.60	.181	5.50	5.74	4.4
1.30	352	61.1	4.90	100.0	14.30	13.60	5.10	.226	4.40	4.54	3.2
1.53	422	73.5	5.90	120.0	17.10	16.10	6.20	.266	3.76	3.86	2.7
1.80	494	86.0	6.90	140.0	20.10	18.90	6.35	.326	3.08	3.28	6.1

Error Average 4.10% Error Average 3.0%

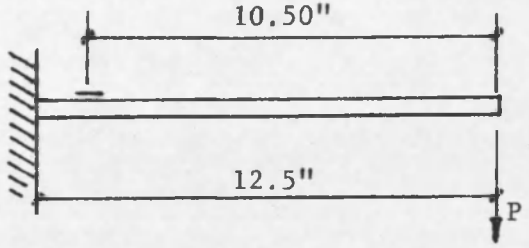

Data: $\alpha = 45^{o}$

$d = .250$ in.

$b = 2.95$ in.

$A_f = .00750$ in.^{2}

Table III. Stress and Deflection Results - Specimen No. 3

P	ϵ''_m	s''_m	s_m	s_f	Eq.(9) M_a	M	% Error	Δ_a	$1/\Delta a$	Eq.(18) $1/\Delta a$	% Error
lbs.	$\frac{\mu in.}{in.}$	psi	psi	psi	in.-lb.	in.-lb.	-	in.	1/in.	1/in.	-
.33	68	11.8	.94	28	3.77	3.46	8.95	.050	20.00	21.00	5.0
.60	120	20.8	1.67	50	6.70	6.25	7.20	.093	10.80	11.60	7.4
1.03	212	36.8	2.94	88	11.70	10.80	7.60	.164	6.10	6.71	10.0
1.30	268	46.5	3.72	111	14.80	13.60	8.80	.206	4.85	5.33	9.9
1.53	315	54.6	4.37	131	17.70	16.10	9.90	.242	4.14	4.53	9.4
1.80	370	64.2	5.13	153	20.50	18.90	8.50	.285	3.50	3.84	9.7

Error Average 8.40%

Error Average 8.50%

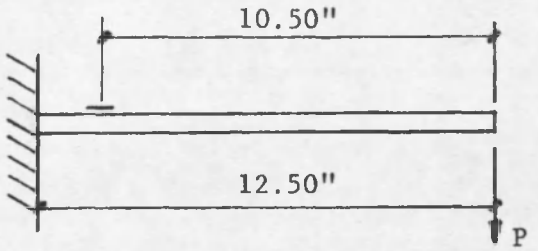

Data: $\alpha = 30^o$

d = .250 in.

b = 3.00 in.

A_f = .00895 in.^{2}

materials through the beam's thickness. These are problems that should be investigated in the future study of this work.

Some explanation of the data presented in Tables I, II, and III is necessary. First, equation (9) has only one unknown, s_f. This term was evaluated as follows:

1. The matrix strain at the outermost top fiber, ϵ''_m, was measured by the strain gages (column 2 of Tables). This measurement was taken at the center of the beam, since it was found that there was only a 5% variation in strain across the beam width (on both 25 ply specimens).
2. The matrix stress, s''_m, was then computed by multiplying ϵ''_m by the matrix Modulus of Elasticity, E_m (column 3).
3. The value of s''_m was then multiplied by the appropriate ratio to give the matrix stress at a level t from the neutral axis, s_m (column 4). This ratio was 2/11 and 2/25 for the 11 and 25 ply specimens respectively.
4. Finally, the corresponding fiber stress, s_f, was computed by using the relationship from equation (6):

$$s_f = s_m \cos^2\alpha \frac{E_f}{E_m}$$

These values are presented in column 5. Having now evaluated s_f, the theoretical moment M was computed by substitution into equation (9). The value of this moment and the actual moment M_a are shown in columns 6 and 7. (M_a = P x L).

It should be noted that the values of the beam length L were different

in the computation of the stress and deflection equations. The value of L used for the stress equation was measured from the center of the strain gages to the point of loading. However for the deflection equation, L was measured from the point where the beam was fixed to the point of loading. Refer to illustrations shown with Tables I, II, and III for further clarification of specimen data used.

Analysis and Conclusions

Figure 23 shows the relationship between load and strain for each of the three specimens. Comparing the curves for the 11 ply and 25 ply beams, it is clearly shown that by increasing the beam depth by a factor of 2.3, the load carrying capacity is increased by a factor of 5.5. This is not surprising considering the fact that the Section Modulus of the beam effectively varies as the square of the depth. However, note the apparent difference in strain between the second and third specimens. Specimen 3 with $\alpha = 30^{\circ}$ shows 33% lower strains than that of specimen 2 with $\alpha = 45^{\circ}$. This is because the third specimen has more fiber area per beam width than does the second. With an α of 30°, the center-to-center spacing of fibers is .0695 $in.^2$ This results in a fiber area of .00895 $in.^2$, as compared to a center-to-center spacing of .085 in. and an area of .0075 $in.^2$ for a specimen with α of 45°. Hence, the larger the percentage of fibers acting in a direction of loading, the higher the load capacity of the composite beam. (The author recognizes the fact that the number of tests were limited and that other angles of α should be tested in the future over a wide range).

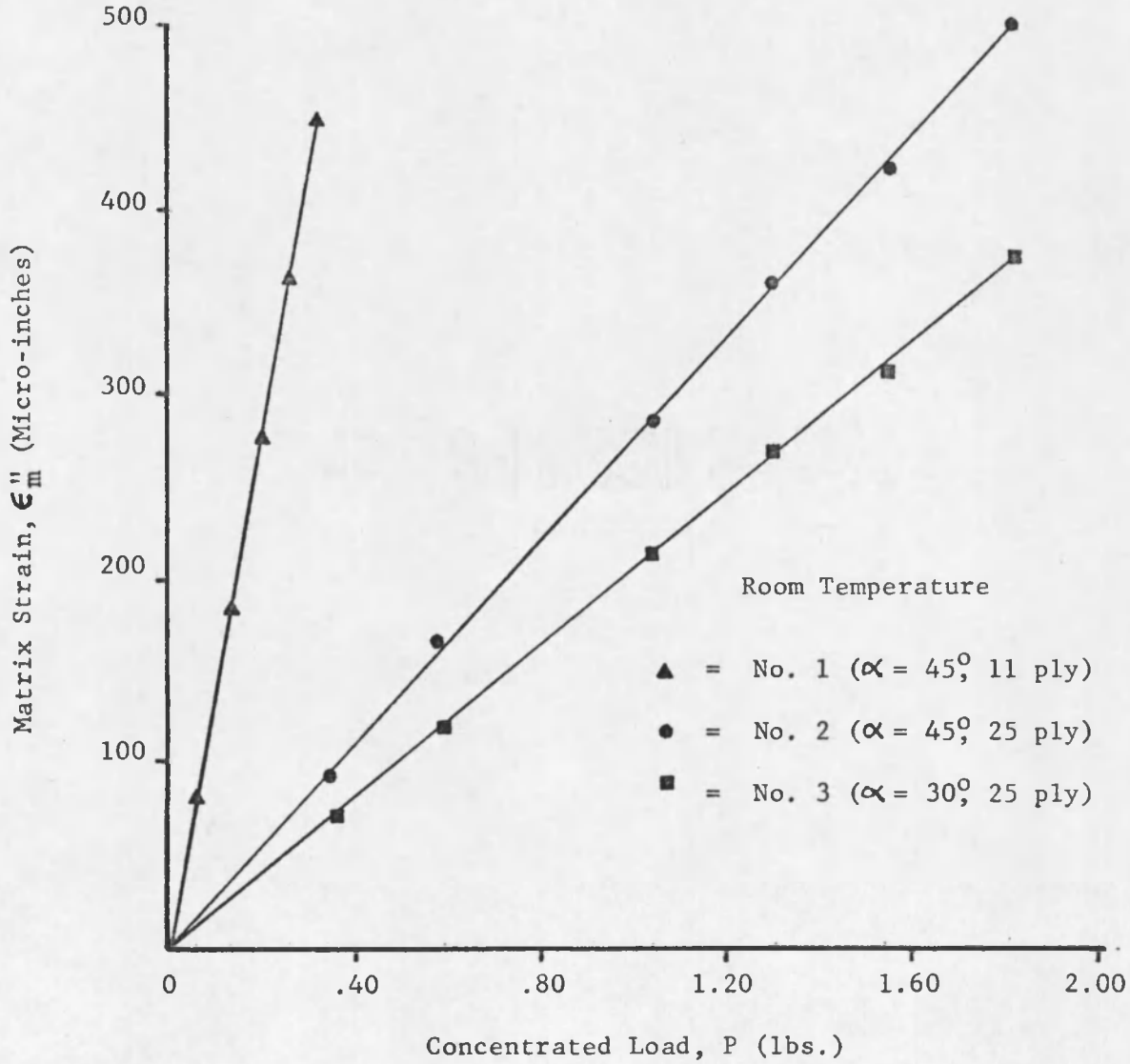

Figure 23. Load-Strain Curves

Figure 24 shows the curves obtained from the load-deflection data. The same type of observations regarding load carrying capacity can be derived from these curves. Namely, that by increasing beam depth and fiber area, deflections are reduced accordingly. Comparing the curves for specimens 2 and 3, it is shown that even though each specimen had the same gross cross sectional area, specimen 3 deflected 14.5% less. This is attributable again to the increased fiber area.

Inspection of the percentage of error figures in Tables I, II, and III shows another significant conclusion. It is that the best results were obtained with specimens having uniform construction characteristics (specimens number 1 and 2). That is, the third specimen was observed to have a slight variation in the angle α on the top as compared with the bottom of the beam. Probably as a consequence, it had the highest percentage of error. Therefore, in order for equations (9) and (18) to be valid in an frp beam, it is imperative that each glass fiber mat be laid down uniformly throughout.

Up to now, equation (9) has been referred to as the stress equation. However, it is not in a form that can be used to evaluate the fiber stress, given a bending moment M. If equation (9) is solved for s_f, then the formula for the maximum fiber stress in a cantilevered fiberglass reinforced beam is given by

$$s_{f_m} = \frac{M \times R}{2Ct\left[A_f(\cos\alpha + \tan\alpha\sin\alpha) + \left(bt - \frac{A_f}{\cos\alpha} - \frac{A_f}{\sin\alpha}\right)\frac{1}{\cos^2\alpha H}\right]} \quad ..(19)$$

where R = proportional factor for converting fiber stress at level t to

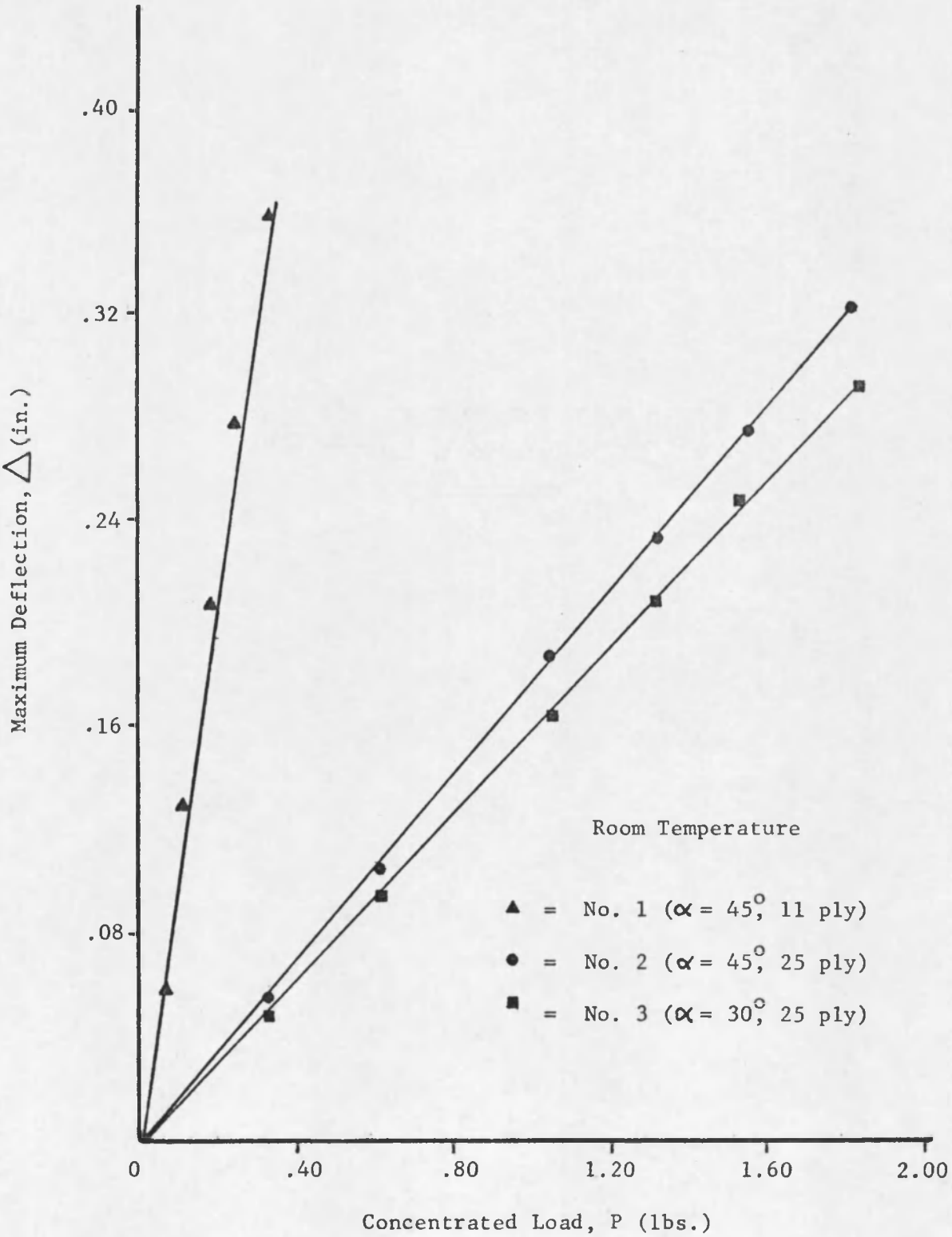

Figure 24. Load-Deflection Curves

maximum outermost fiber stress:

$$R = \frac{\text{total number of plys}}{2} \quad \text{and}$$

$$C = \sum_{k=3,5,7\ldots}^{n} \left(\frac{k-1}{2}\right)^2$$

where n is the number of plys in the beam depth. And

$$H = \frac{E_f}{E_m}$$

Equation (18) is in a usable form and can be used directly to solve for the maximum reciprocal beam deflections. (The reader should refer to the Appendix for sample calculations involving equations (9) and (18). Thus, equations (9) and (18) are acceptable design equations for flexure and deflection due to uniaxial loading on an frp beam subjected to short time loading.

Observation of the deflection data shows some additional final conclusions:

1. Measurements on both sides of the 25 ply beams showed that no significant torsional strains occurred. This is reasonable since the resultant transverse component of fiber forces is zero in any layer.
2. From the deflection calculations, it was found that most of the load (approximately 85%) was carried by the reinforcing.

CHAPTER V

RECOMMENDATIONS FOR FUTURE STUDY

The topics of study in reinforced fiberglass plastics are numerous and challenging. One sequel of this thesis should be the study of time dependent stress-strain relationships and their effects upon the stress and deflection equations. Under static loading conditions, the internal accommodations of the material to plastic flow (creep) influences the breaking strength in a way that cannot be predicted by the type of short time test that were incorporated in this study. Therefore, creep-rupture tests could be run on frp to evaluate a valid criteria for strength properties of fiberglass reinforced plastics.

Another topic for continued study should be the development of an equation for torsion. Torsion exists as a result of the shear component of the fiber stress in the transverse direction of the beam. Although little twisting was observed in our specimens, there could be a situation where significant torsion would occur.

Other possible areas of investigation in the field of frp include the following:

1. Find the Modulus of Elasticity of a single roving of glass fiber. Impregnation of the glass in a matrix of polyester resin having a small diameter is a suggested method.
2. Investigate the use of cotton fabric in place of fiberglass as the reinforcing material.

3. Investigate the strength properties of an frp beam made up of randomly orientated roving fibers.
4. Develop design equations for shear.
5. Conduct a study on the impact resistance of fiberglass reinforced plastics.
6. Conduct a study on adhesive bonding of frp to other structural parts such as wood, steel, etc.

APPENDIX

SAMPLE CALCULATIONS OF STRESS AND DEFLECTIONS

The calculations shown in this section are for specimen number 2. The solution of equation (9) is presented first.

Beam data:

$\alpha = 45^{o}$ $\quad E_m = 174{,}000$ psi

$d = .250$ in. $\quad E_f = 7{,}000{,}000$ psi

$b = 2.95$ in. $\quad L = 10.5$ in. (eq. (9))

$n = 25$ plys $\quad L = 12.5$ in. (eq. (18))

$A_f = .00750$ in.^{2}

Since $d = .250$ in., and there are 25 plys in the beam depth, then

$$t = \frac{.250 \text{ in.}}{25} = .0100 \text{ in.}$$

Direct substitution of data into equation (7) gives the solution of P_y.

$$P_y = s_f((.0075 \times .707) + (.0075 \times 1 \times .707)) + \ldots$$

$$\ldots (2.95 \times .001 - \frac{.00750}{.707} \times 2)\, s_m \qquad \text{or}$$

$$P_y = .0106 s_f + .007 s_m$$

Therefore, given the test values of s_f and s_m, a numerical answer may be obtained for P_y. (Refer to Table II for stress data). Now the expression for equation (9) becomes

$$M = 2(.001)P_y \left[1^2 + 2^2 + 3^2 + \ldots + 11^2 + 12^2\right] \quad \text{or}$$

$$M = 2(.001)P_y(650) = 13.0\ P_y$$

Thus for any value of P_y, the value of the theoretical moment can be evaluated. Now to arrive at a solution for the reciprocal of the beam deflection (equation (18)), first solve for I_f'.

$$I_f' = \frac{2 \times .0075}{.707}\left[\overline{12(.01)}^2 + \overline{11(.01)}^2 + \ldots + \overline{2(.01)}^2 + \overline{1(.01)}^2\right]$$

$$= .0212(.0650) = .00138 \text{ in.}^4$$

The matrix moment of inertia I_m is then

$$I_m = \frac{2.95 \times .250^3}{12} - .00138 = .00246 \text{ in.}^4$$

The term I_f can next be evaluated

$$I_f = \frac{.0075(.0650)}{.707} = .00069 \text{ in.}^4$$

Substituting the appropriate terms into equation (18) gives

$$\frac{1}{\Delta_t} = \frac{(3)(174{,}000)\ (.00246)}{P \times (12.5)^3} + \frac{(3)(1.414)(.707)^2(.00069)(7{,}000{,}000)}{P \times (12.5)^3}$$

$$\frac{1}{\Delta_t} = \frac{.65}{P} + \frac{5.25}{P} = \frac{5.90}{P}$$

Thus given the value of P (in pounds), the reciprocal of the maximum beam deflection can be solved.

REFERENCES

1. Browne, H. C. "Structural Applications of Plastics Past, Present, Future," Paper Presented at Kansas City Convention - American Society of Civil Engineers (Structural Division) 1965.

2. Baer, Eric, ed. "Reinforced Plastics," in Engineering Design for Plastics. New York: Reinhold Publishing Corp., 1964. 869-994.

3. Duffin, D. J. Laminated Plastics. New York: Reinhold Publishing Corp., 1966.

4. Browne, H. C. "Plastics in Construction," Civil Engineering. Vol. 39, (August 1969), 39-41.

5. Unpublished Air Force Design Manual for Plastics, in Preparation by the Department of Civil Engineering, Syracuse University, 1967. (Copy available from Professor Haaren A. Miklofsky).

6. Sonneborn, Ralph H. Fiberglass Reinforced Plastics. New York: Reinhold Publishing Corp., 1954.

7. Schwartz, R. T. Fundamental Aspects of Fiber Reinforced Plastic Composites. New York: Interscience Publishers, 1968.

8. Riddle, Malcolm N. "Significant Properties of Plastics for Design," Paper presented at Louisville, Ky. Convention - American Society of Civil Engineers (Structural Division) 1969.

9. Timoshenko, S. Elements of Strength of Materials. 3rd ed., New York: D Van Nostrand Co., Inc., 1949. 166-167.

10. Miklofsky, Haaren A. Studies of Bending Interaction: Suspension Bridges. Dissertation Presented to Faculty at Yale School of Engineering, 1950.